Expanded View Figures

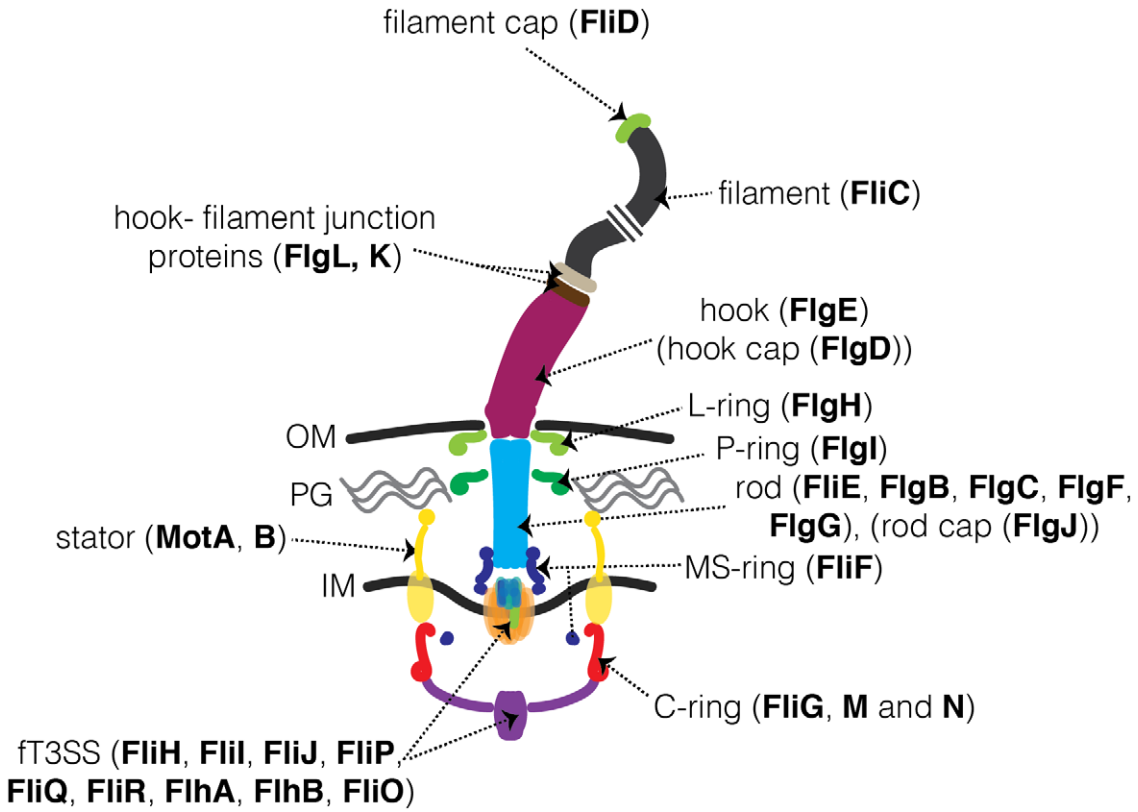

Figure EV1. Schematic of the *Escherichia coli* flagellar motor.

A schematic representation of the *E. coli* flagellum highlighting its major parts and their constituent proteins. The same color code is used in all main and supplemental figures, except Appendix Fig S3.

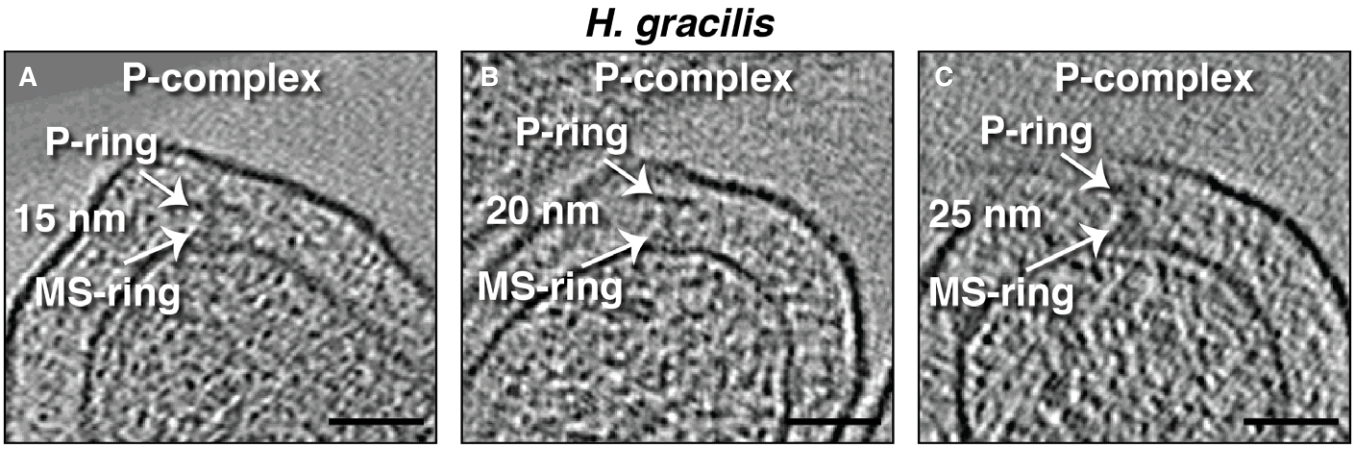

Figure EV2. The variable position of the P-ring in *Hylemonella gracilis* P-complexes.

A–C Slices through electron cryotomograms of *H. gracilis* showing P-complexes. The variable distance between the MS- and P-rings is indicated (15, 20 and 25 nm, respectively). Scale bars are 50 nm.

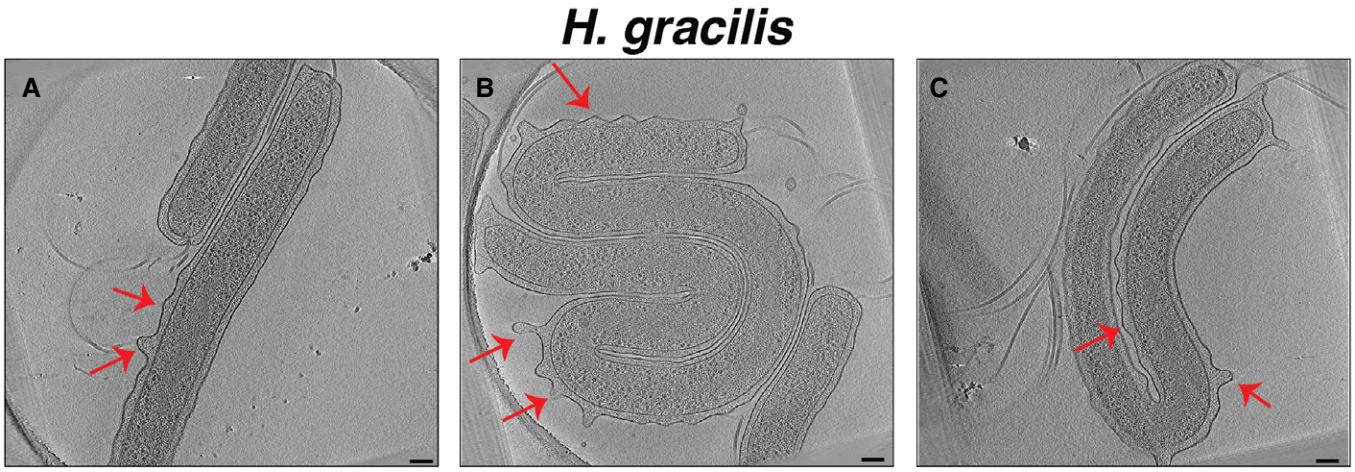

Figure EV3. The undulating outer membrane of *Hylemonella gracilis*.

A–C Slices through electron cryotomograms of *H. gracilis* highlighting undulating OM (indicated by red arrows). Scale bars are 100 nm.

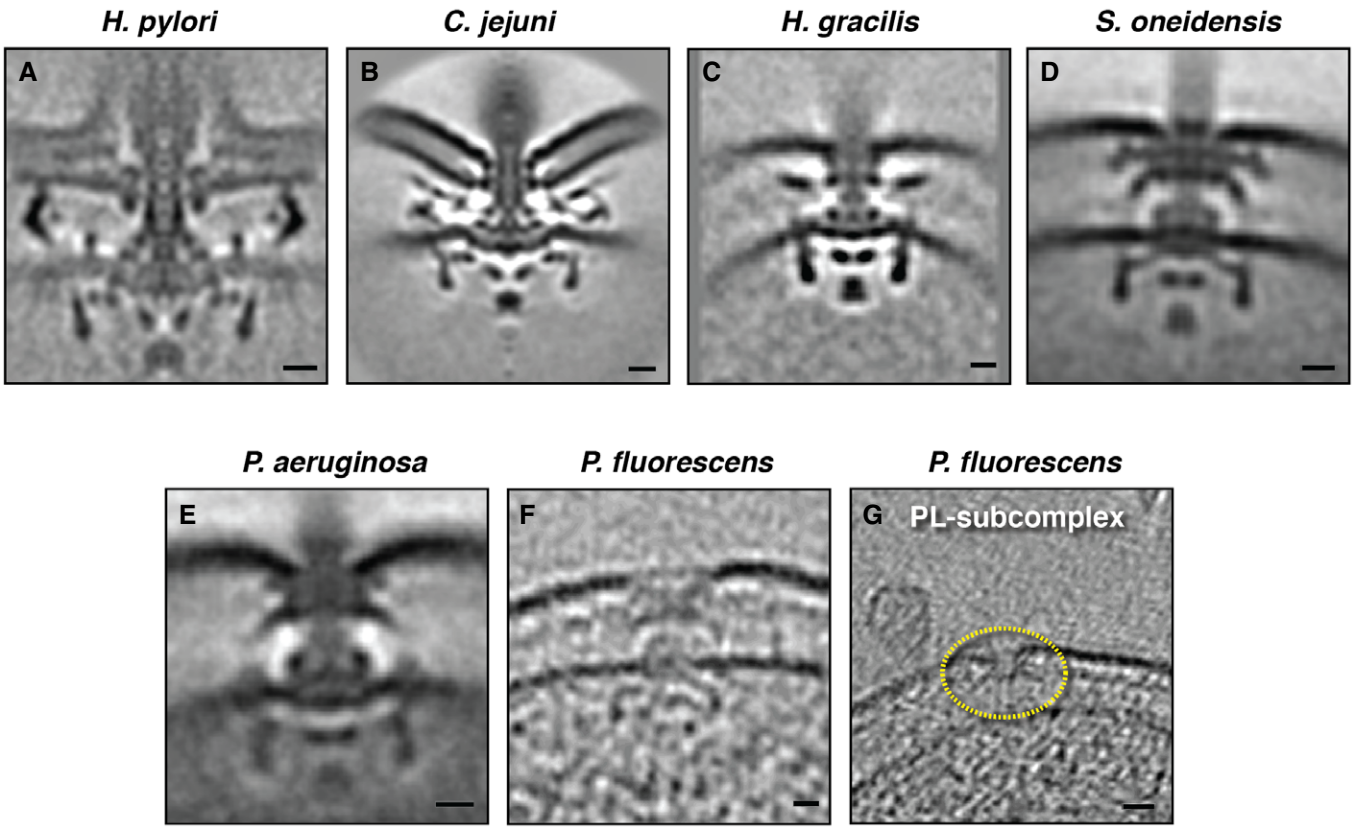

Figure EV4. The flagellar motors of the species investigated in this study.

A–E Central slices through the STAs of fully assembled high-torque motors in species in which we identified novel cytoplasmic rings interacting with the FliG ring during assembly. The *H. pylori* motor is from (Qin *et al*, 2017), *C. jejuni* motor from (Beeby *et al*, 2016), *S. oneidensis* and *P. aeruginosa* motors from (Kaplan *et al*, 2019a).

F, G Slices through electron cryotomograms of *P. fluorescens* highlighting the presence of a basal body (F) and a disassembly PL-subcomplex (G, yellow dotted circle), showing the similarity of the motor of this species to that of *P. aeruginosa*.

Data information: Scale bars (A–F) 10 nm, (G) 20 nm.

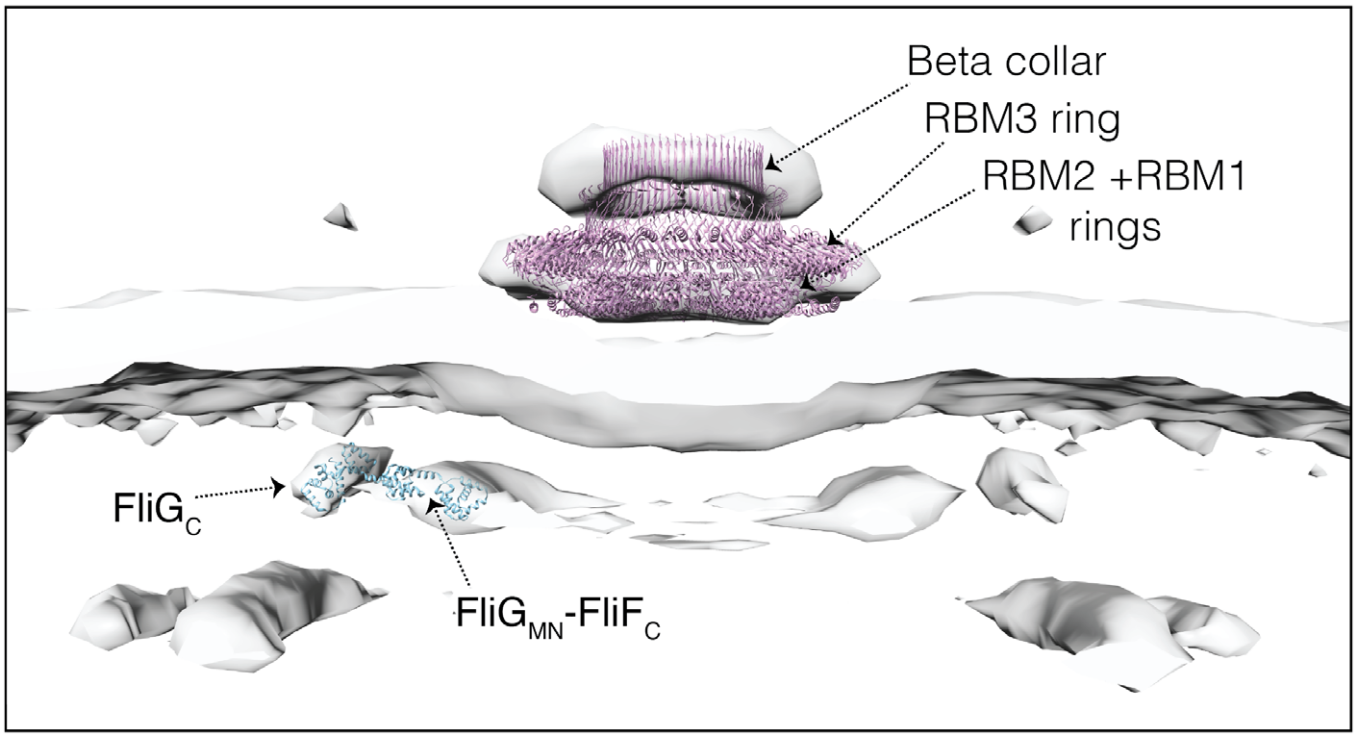

Figure EV5. Tentative component assignment to various MS-complex rings in *Helicobacter pylori*.

Surface rendering of the MS-complex of *H. pylori fliP** with the crystal structures of *Aquifex aeolicus* FliG (PDB 3HJL) and *S. enterica* MS-ring (PDB 6SCN) docked inside it. RBM, ring-building motif.